AN EXPERIMENTAL INVESTIGATION OF THE SEPARATING/REATTACHING FLOW OVER A BACKSTEP

Progress Research Report

Cooperative Agreement No.: NCC2-465

for the period

March 1, 1992 - January 31, 1993

Submitted to

National Aeronautics and Space Administration
Ames Research Center
Moffett Field, California 94035

Experimental Fluid Dynamics Branch
Joseph G. Marvin, Chief
David M. Driver, Technical Officer

Fluid Dynamics Division
Paul Kutler, Chief

Prepared by

ELORET INSTITUTE
1178 Maraschino Drive
Sunnyvale, CA 94087
Phone: 408-730-8422 and 415-493-4710
Telefax: 408-730-1441
K. Heinemann, President and Grant Administrator
Srboljub Jovic, Principal Investigator

31 January, 1993

INTRODUCTION

This progress report covers the grant period from March until the end of January 1993.

Extensive data reduction and analysis of single and two-point measurements for a backward-facing experiment were performed. Pertinent results are presented in two conference papers which are appended to this report.

The titles of the papers are as follows:

1. "Two-point correlation measurements in a recovering turbulent boundary layer", to be presented at the International Conf. on Near Wall Turbulent Flows, March 15-17, 1993, Tempe, Arizona.

2. "An experimental study on the recovery of a turbulent boundary layer downstream of the reattachment", to be presented at the 2nd International Symposium on Engineering Turbulence Modelling and Measurements, May 31- June 2, 1993, Florence, Italy.

International Conf. on Near-Wall Turbulent Flows, March 15-17, 1993, Tempe, Arizona, USA

Two-point correlation measurements in a recovering turbulent boundary layer

Srba Jovic

Eloret Institute, 3788 Fabian Way, Palo Alto, CA 94303

Abstract

Space-time correlation and the shear stress conditional quadrant decomposition techniques were used to assess the structure of a turbulent boundary layer. The boundary layer was recovering from the strong perturbation produced by a backward-facing step. All two-point, two-component, velocity measurements were conducted 38 step-heights, h, downstream from the step. It is found that the structure of the recovering boundary layer is dominated by an attached double-cone eddy in the near wall region and by a double-roller eddy in the outer flow. The postulated structure is more elongated in the cross coordinate directions of the recovering boundary layer when compared to the one found in a regular flat-plate zero-pressure gradient turbulent boundary layer. The conditional quadrant analysis have revealed that the shear stress production is dominated by the Q_2 and Q_4 events while the contribution by the interactive events, Q_1 and Q_3, remains relatively small. It appears that the Q_1 and Q_3 motions are largely induced by the very energetic Q_2 and Q_4 events.

1. INTRODUCTION

Two-point correlation measurements have proven to be a very powerful tool in the analysis and quantification of organized structures in turbulent flows. There are basically two schools of thought about how to use two-point measurements for deduction of organized structures. One approach, deductive in nature, checks the consistency of a proposed organized structure with measured two-point correlation profiles. Townsend (1956,1976) was the first to demonstrate this approach using Grant's (1958) two-point measurements in the turbulent wake behind a circular cylinder and in the flat-plate turbulent boundary layer (TBL). The results of this technique were revolutionary at a time, when they gave birth to the concept of the double-roller eddy structure in the wake flow and the attached eddy in the TBL. The second, inductive, approach has been introduced by Lumley (1967). He proposed the proper orthogonal decomposition (POD) technique to objectively identify and extract the organized structure of a turbulent flow. This method uses an orthogonal decomposition to obtain eigenmodes from two-point correlation profiles. An organized structure is identified as the most energetic eddy and is uniquely defined as the eigenfunction with the largest eigenvalue. These eigenfunctions can be subsequently used to reconstruct an associated flow structure and obtain its contribution to the Reynolds stress tensor. Using the POD technique, Payne (1966) utilized Grant's (1958) two-point measurements to find that

the dominant structure in a turbulent wake is the double-roller eddy. Bakewell & Lumley (1967) utilized the POD to obtain a pair of counter rotating eddies in the wall region of the turbulent pipe flow. Both findings are consistent with Townsend's (1956,1976) proposed structural models.

The objective of this investigation is to deduce the flow structure of a recovering turbulent boundary layer using two-point two-component velocity measurements based on their similarity with the measurements of Grant (1958) and Tritton (1967). In addition, new potentials of two-point measurement are exploited using quadrant decomposition and conditional quadrant decomposition of the shear stress.

2. EXPERIMENTAL ARRANGEMENT AND CONDITIONS

The experiment was performed in the 20x40*cm* low-speed open-circuit wind tunnel at the NASA Ames Research Center. The boundary layer was tripped at the end of the contraction to promote regular transition. The fully developed turbulent boundary layer was perturbed 169*cm* downstream from the trip by a backward-facing step of the height, h, of 38*mm*. The aspect ratio W/h, where W is the wind tunnel width, was 11 while the duct area expansion ratio was 1.19. The reference velocity, U_{ref}, measured at a reference point upstream of the step was $10.0m/s$ which corresponded to a Reynolds number based on the step-height, R_h, of 25500. The free stream turbulence level in the tunnel was 0.4% measured at $10.0m/s$. The boundary layer thickness, $\delta \equiv \delta_{99}$, upstream of the step was 30*mm* which yielded $\delta/h=0.77$ with a Reynolds number based on the momentum thickness, R_θ, of 2000. The separated flow reattaches at $6.7h$ downstream from the step. The free stream velocity, U_e, of the recovering boundary layer at $x/h=38$ was $8.9\ m/s$, the boundary layer thickness, δ, was 110 *mm*, the momentum thickness, θ, was 12 *mm*, the shape factor, H, was 1.3 and the Reynolds number, R_θ, was 7100.

Turbulence measurements were performed with a set of constant-temperature anemometers used in conjuction with X-wire probes. The sensor filaments were made of 10% Rhodium-Platinum wire, 2.5μm in diameter and 0.6mm long, which resulted in an aspect ratio, l/d, of 240 and normalized length, $l^+ = lu_\tau/\nu$, of 14.5. The frequency response of the constant-temperature anemometer was 50kHz. Data were collected by a microVax II computer interfaced with a high speed sample-and-hold Tustin A/D converter which was set at 6000 *Hz*. The record length of each channel was 30 *sec*.

Instantaneous turbulent velocity fluctuations u and v were measured in the streamwise, x, and normal, y, directions respectively. The z-axis is in the spanwise direction of the flow. The subscripts 1, 2, 3, will also be used to refer to the x, y and z directions respectively.

3. RESULTS AND DISCUSSION

3.1 Mean flow characteristics

All the measurements were performed at a fixed streamwise location $x/h=38.55$. The two dimensionality of the mean flow was checked by the spanwise measure-

ments of the mean velocity component, U, and the shear-stress coefficient C_f. It was found that the velocity distribution was uniform in the z-direction to $\pm$ 2% measured at y/δ= 0.45 while C_f distribution was uniform to $\pm$4% for -δ to δ about the symmetry plane of the tunnel.

The wall stress was measured directly using laser oil interferometry. The measured skin friction coefficient, C_f=0.003, was used to normalize the mean streamwise velocity. It was compared against the universal law-of-the-wall velocity distribution, $U^+\equiv U/u_\tau = 1/0.41\ \ln y^+ + 5.1$, shown in Figure 1(a). It appears that the velocity distribution agrees well with the logarithmic velocity distribution in the near-wall region up to $y^+=u_\tau y/\nu$ of about 200 or y/δ= 0.08. However, it dips below the universal log-law distribution for greater values of y^+. This resulted in the larger value of Prandtl's mixing length in the outer part of the recovering boundary layer, and in the larger slope in the inner layer. Cutler & Johnston (1989), Jovic & Browne (1990) and Jovic (1993) have observed values of the mixing length in the outer layer which are about two times larger than those in a regular TBL.

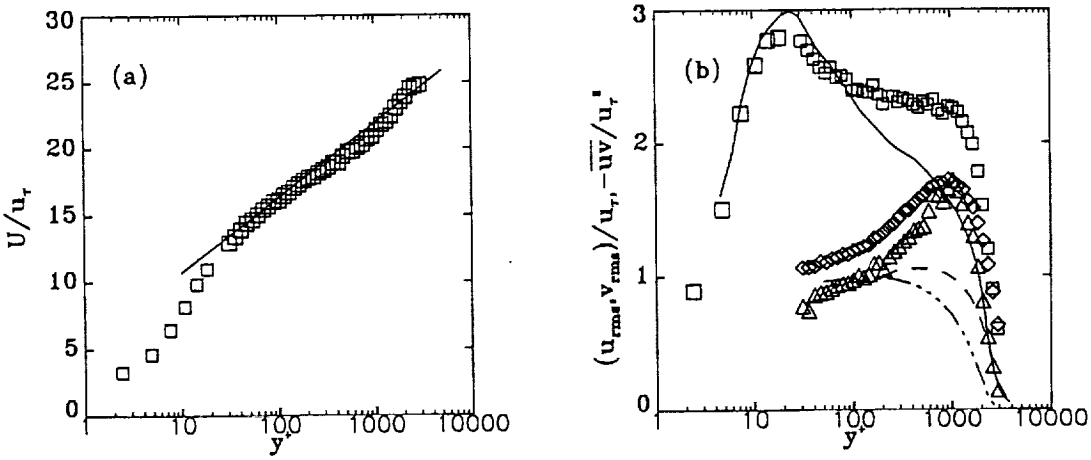

Figure 1. (a) Mean velocity profile and (b) turbulence intensities and shear stress. Symbols: (a) —, $U^+=1/0.41\ \ln y^+ + 5.1$, (b) ❑, u_{rms}/u_τ; ◊, v_{rms}/u_τ; Δ, $-\overline{uv}/u_\tau^2$. Klebanoff's experiment: —, u_{rms}/u_τ; – –, v_{rms}/u_τ; ...—, $-uv/u_\tau^2$

Turbulence intensities u_{rms} and v_{rms} and the shear stress, $-\overline{uv}$, profiles are shown in Figure 1(b). It appears that the streamwise turbulence, u_{rms}, agrees well with Klebanoff's (1954) measurements in the inner layer. Using the transport equation of the turbulent kinetic energy, Jovic (1993) showed that the near-wall structure of this flow has nearly recovered to an equilibrium state at this x location unlike the outer part of the flow. It was further shown that the structure in the near-wall and the outer flow regions have different rates of recovery. The near-wall structure recovers much faster and attains a quasi-equilibrium state for x/h>30 while the outer turbulent structure takes presumably 100h to recover to a flat-plate TBL structure.

3.2 Results of correlation measurements

Correlation between two quantities p and q at two spatial points **x** and **x+r** is

defined as

$$R_{pq}(x,r) = \frac{\overline{p(x)\,q(x+r)}}{\sqrt{\overline{p^2(x)}}\sqrt{\overline{q^2(x)}}}$$

where **x** denotes the position vector of the fixed (or reference) probe and **r** is the separation vector. The first subscript, p, in R_{pq} denotes a quantity at a reference point and the second one, q, denotes a quantity at a location of the moving probe. Four different correlations were considered, i.e. $R_{uu}(\mathbf{x},\mathbf{r})$, $R_{vv}(\mathbf{x},\mathbf{r})$, $-R_{uv}(\mathbf{x},\mathbf{r})$ and $-R_{vu}(\mathbf{x},\mathbf{r})$. The present discussion will be confined to cases where the separation vector was $\mathbf{r}= (0, r_2, 0)$ or $(0, 0, r_3)$, i.e. when the moving probe is moved in the normal, y, or spanwise, z, direction keeping the streamwise location, x, constant and equal to that of the stationary probe. In this case the notation can be abbreviated to $R_{pq}(r_2)$ and $R_{pq}(r_3)$ respectively. Note that $R_{pq}(0)$ is equal to unity in the case when $p \equiv q$ and to the local correlation coefficient when $p \neq q$. Any departure from these values can be attributed to a finite initial displacement of probes. Measurements were performed for four different y locations of the stationary probe, namely y/δ= 0.012,0.2,0.38 and 0.75 (y^+= 30, 510, 965 and 1905 respectively). The stationary probe was located at $z/\delta = 0.45$ off the plane of symmetry of the tunnel for all z traverses. For the z traverse in the wall region, the stationary probe was moved to a slightly larger distance from the wall, namely, to y/δ=0.018 (y^+=45). Two y/δ locations, 0.012 and 0.38, were selected because $\overline{u^2}$ attains a maximum (or nearly a maximum) values at these locations in the inner and the outer layers of the recovering boundary layer.

Correlations $R_{uu}(r_2)$, $R_{vv}(r_2)$, $-R_{uv}(r_2)$ and $-R_{vu}(r_2)$ for different distances from the wall are shown in Figure 2. All four correlations are virtually non-negative for r_2 separations. The correlation $R_{uu}(r_2)$ for y/δ=0.012 remains non-zero for very large r_2 separations approaching zero value at about r_2/δ=0.85 as seen in Figure 2(a). For the same distance of the reference probe from the wall, $R_{uu}(r_2)$ decays rapidly for small r_2 suggesting the presence of structures of smaller length scales near the wall. The extent of the strong correlation over larger r_2 separations implies presence of unusually large structures in the outer part of the flow which appear to communicate with the near-wall flow structure. It appears that $R_{uu}(r_2)$ for the two different distances from the wall, y/δ=0.20 and 0.38, are identical for positive r_2 (see Fig. 2(a)), suggesting that length scales in the outer layer are constant. However, the correlation falls off rapidly for negative r_2, particularly when the stationary probe is closer to the wall. For the stationary probe located at y/δ=0.012, $R_{vv}(r_2)$ decreases rapidly in the y direction, falling to a value of almost zero at r_2/δ=0.2 and remaining virtually zero for the rest of the boundary layer. For larger distances of the stationary probe from the wall, $R_{vv}(r_2)$ exhibit surprisingly high magnitudes suggesting that motions associated with the v fluctuating component are of much larger length scales then those found in the flat-plate TBL of Grant (1958) and Tritton (1967). It appears that $R_{vv}(r_2)$ is identical for positive r_2 (see Fig.2(b)) for the two characteristic positions of the reference probe (y/δ=0.20 and 0.38) as in the case of $R_{uu}(r_2)$. Reduced size of structures near the wall leads to a rapid decay of $R_{vv}(r_2)$ for negative r_2. Comparison of $R_{uu}(r_2)$ and $R_{vv}(r_2)$

with classic measurements of Grant (1957) and Tritton (1967) (not shown) shows that u and v fluctuating components are strongly correlated over much larger r_2 separations in the present experiment then in the case of a regular TBL. It appears that the length scales of the recovering boundary layer at the given x location are roughly two times larger then those of a flat-plate TBL. Correlations $-R_{uv}(r_2)$ and $-R_{vu}(r_2)$ are not identical for y traverses as seen from Fig. 2(c) and (d). However, they should be identical for r_2=0 and the reason why they are not is because of the finite initial spanwise separation of the two probes. The correlation $-R_{vu}(r_2)$, for y/δ=0.012, decays rapidly for increasing r_2 separations, approaching zero at about r_2/δ=0.45. For larger distances from the wall $-R_{vu}(r_2)$ falls less dramatically showing that u and v are well correlated further from the wall.

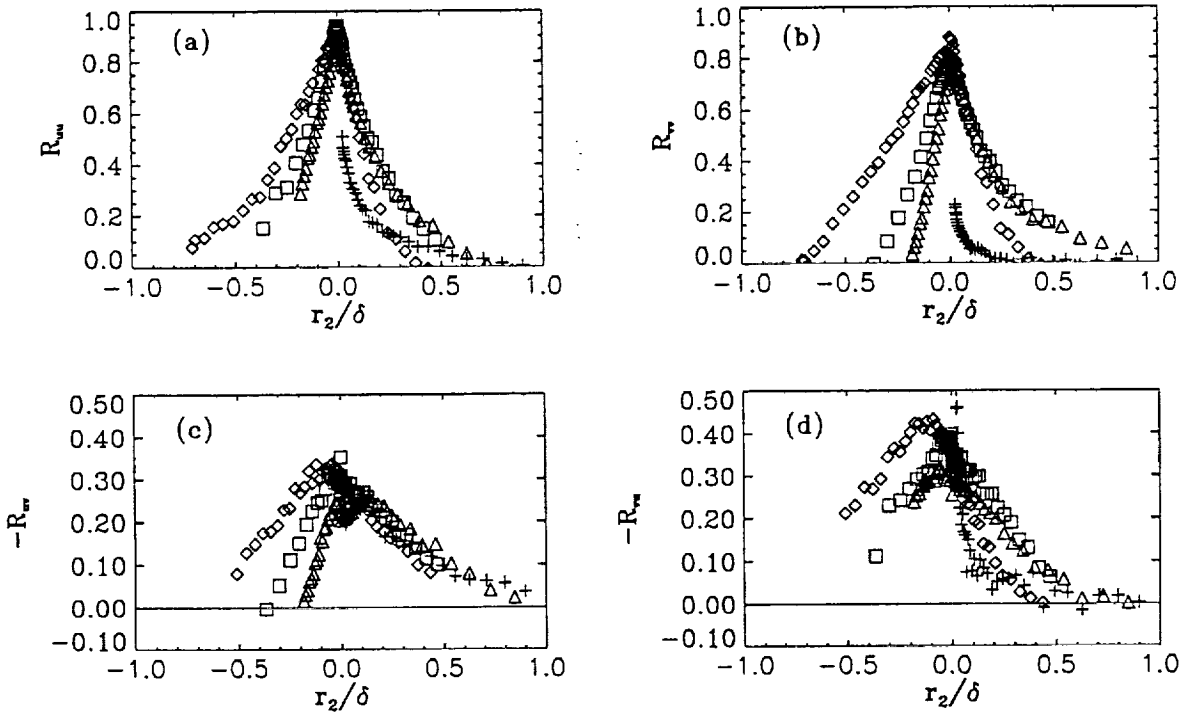

Figure 2. Space correlations for r_2 separations for four different y locations of stationary probe. Symbols: +, y/δ=0.012; Δ, y/δ=0.20; ❑, y/δ=0.38; ◊, y/δ=0.75.

Figure 3 shows four correlations for r_3 separations for the four different distances of the reference probe from the wall. The most striking point observed in their behavior is the change of the sign. The change of the sign suggests periodicity in the z direction. The separation at which the minimum of the $R_{uu}(r_3)$ profile occurs provides an estimate of an average separation between the high and low speed fluid. Near the wall (reference probe was at y/δ=0.018), $R_{uu}(r_3)$ decreases rapidly for r_3/δ<0.05 indicating the presence of motions of much smaller scales than those for the larger distances from the wall (Fig.3(a)). However, the rate of decay of $R_{uu}(r_3)$ reduces for separations r_3/δ>0.05 eventually falling off to zero value at r_3/δ=0.35. This two-component form of the correlation profile close to the wall according to Townsend (1956) suggests the presence of two distinct ranges of

eddy sizes. Minimum values of R_{uu} occur at about r_3/δ=0.6 for the reference probe at y/δ=0.20 and 0.38 and at r_3/δ=0.7 for y/δ=0.75. Apparently the spanwise spacing of the high/low speed streaks gradually increases with the normal direction. Close to the wall, $R_{vv}(r_3)$ becomes negative for r_3 which are smaller than those of the other correlations. The negative values of $R_{vv}(r_3)$, together with the occurrence of the minimum, suggest the presence of streamwise vortical structures. The negative lobe of R_{vv} almost disappears away from the wall for y/δ>0.38.The separation of the minimum from the origin can be interpreted as an average diameter of a characteristic streamwise vortex. The R_{vv}, $-R_{uv}$ and $-R_{vu}$ correlations close to the wall decrease very rapidly so that due to the lack of the spatial resolution in this region the decreasing limbs of the correlation functions have not been properly resolved.

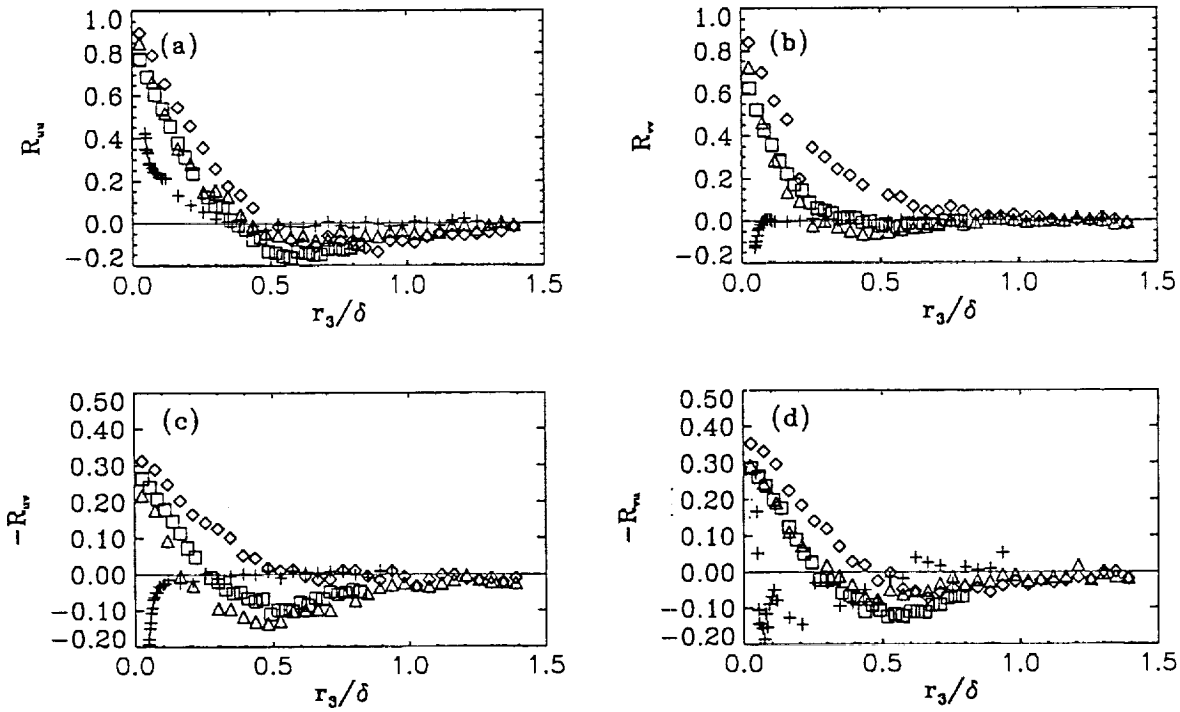

Figure 3. Space correlation for r_3 separations for four different y locations of stationary probe. Symbols: +, y/δ=0.018; Δ, y/δ=0.20; ❑, y/δ=0.38; ◊, y/δ=0.75.

Measured space correlations are similar to those measured in a flat-plate turbulent boundary layer by Grant (1958) and Tritton (1967). However, the turbulent quantities of this flow correlate over greater spatial separations in both y and z directions suggesting that there are larger scales of motion in this flow then in a flat-plate TBL. This provides indirect evidence that the large scale organized structures present in the recovering boundary layer are similar to the Townsend's attached double-cone and double-roller eddies in the near- wall and outer layers respectively, however, with larger y and z dimensions. The two characteristic structures can be connected to form a hairpin structure as shown in Figure 5. Space-time correlations will lend some more evidence in favor of the above

hypothesis.

Space-time correlations for the stationary probe located near the wall at y/δ=0.012 are shown in Figure 4. The phase shift seen in $R_{uu}(r_2,\tau)$ increases as the moving probe moved away from the wall. Favre, Gaviglio & Dumas (1957) were the first ones to observe the same phenomenon in their two-point space-time correlation measurements. Their measurements were consistent with Grant's (1958) outward moving "jets" of his large eddy model. Brown and Thomas (1977), using an array of hot wires and wall shear stress probes, have shown that this increasing time delay with distance from the wall is due to the presence of the large coherent structures spanning an entire boundary layer at an inclined angle. This is consistent with the findings of Head & Bandyopadhyay (1981) who have observed hairpin vortical structures in the outer region of a boundary layer using a flow visualization technique. Using the conditional sampling technique, Jovic & Browne (1989) have shown the presence of the inclined δ-structure in the reattached turbulent boundary layer at x/h=17 of the same backward-facing step flow. They have interpreted this structure as a hairpin like vortex. There is a striking difference between $R_{uu}(r_2,\tau)$ and $R_{vv}(r_2,\tau)$ (see Fig. 4(b)). It is normally expected that one would observe a time delay in all space-time correlations due to the intermittent passage of large organized motions which span the flow at an angle relative to the wall. Instead, the $R_{vv}(r_2,\tau)$ shows no time shift for different r_2 separations.

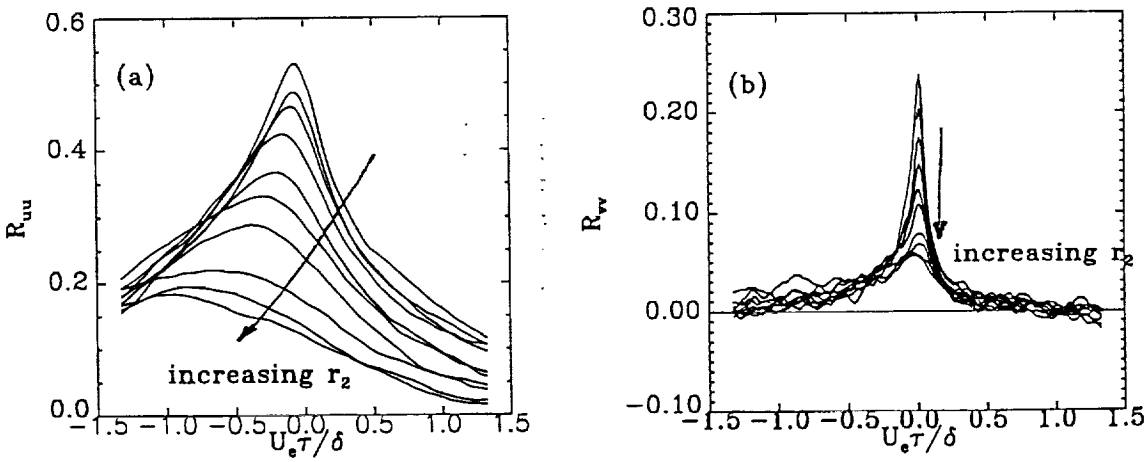

Figure 4. Space-time correlation for r_2 separations for stationary probe at y/δ=0.012.

Observed time delays of the maximum space-time correlations for different r_2 separations (Fig. 4(a)) can be used to reconstruct the spatial form of the detected energetic structure across the boundary layer. It is well accepted that a structure is convected at a nearly constant speed across an entire boundary layer thickness. The convection velocity is approximately U_c=0.8U_e. A possible qualitative model of an organized structure in the recovering TBL is presented in Figure 5. Taylor's hypothesis of "the frozen turbulence" and the convection velocity, U_c, were used to determine the angles of the postulated structure with respect to the x-axis. The

hypothesis of "the frozen turbulence" and the convection velocity, U_c, were used to determine the angles of the postulated structure with respect to the x-axis. The obtained angle in the near-wall, high shear, region is in the range of $\varphi_1=15^0$ to 20^0 which agrees remarkably well with angles obtained by other experimentalists. In the outer layer, the angle is in the range of $\varphi_2= 40^0$ to 70^0 which is somewhat larger than those for a flat-plate TBL. It is deduced that the blending between the two layers occur in the region of $y/\delta\cong 0.2$. The proposed model of the organized structure in the recovering TBL is shown in Figure 5. Based on the two-point space-time correlations, R_{pq}, for r_2 and r_3 separations of the moving probe, presented above, and on their similarities with the results of the cited experiments, it was deduced that the dimensions of the postulated structure are about two times larger in the normal and the spanwise directions than that of the flat-plate TBL.

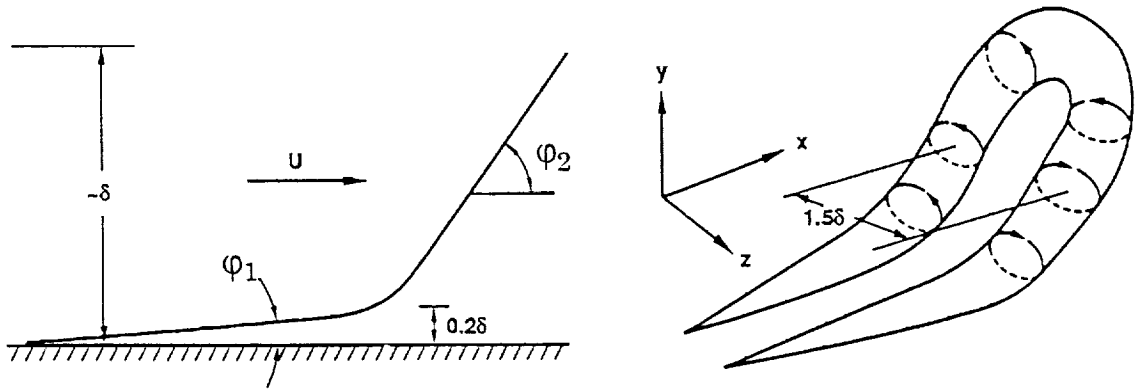

Figure 5. Proposed model of the organized structure in the recovering TBL.

3.3 The conditional quadrant analysis of the shear stress

Simultaneous two-point measurements were used for the conditional quadrant analysis of the shear stress which can lead to a better understanding of the production mechanisms in TBLs.

The conditional probability that the event Q_i (i=1,2,3,4) at the location of the moving probe occurs given that the event Q_j (j=1,2,3,4) has occurred at the stationary point is defined as

$$P_{ij} = P(Q_i \cap Q'_j) / P(Q'_j)$$

and the associated conditional quadrant contribution of the Reynolds shear stress at a moving point is denoted as $\langle uv\rangle_{ij}/\overline{uv}$ corresponding to a Q_{ij} event. For example, if a Q_2 event is observed at the stationary point of a two-point measurements there are four possible events which may occur at the location of the moving point, i.e. shear stress can be in either of the four quadrants.

Hence, the probability, P_{i2}, of Q_i given that the Q_2 has occurred at a given fixed point is obtained together with the associated $\langle uv\rangle_{i2}/\overline{uv}$ where i=1,2,3,4. A conditional quadrant decomposition is shown in Figure 6 for the fixed probe at $y^+=30$ ($y/\delta=0.012$). As can be seen from Figure 6, the conditional interactive motions, Q_{1i} and Q_{3i}, are relatively weak and spatially limited. It appears that the interactive motions are independent of the condition at the reference probe for $y/\delta>0.2$. However, Q_{14} and Q_{32} motions near the wall appear to be well correlated with Q_4 and

streamwise vortices and a Q_2 events as argued by Moin & Kim (1982) and Kim (1983). In addition, Q_3 interactive motions in the wall region might be due to the deflection of ejections which produce Q_2 events. A dramatic change in the contributions to the shear stress by the different quadrants is observed when Q_2 and Q_4 are chosen as conditions at the reference probe near the wall (Figs 6(b),(d)). The positive $\langle uv\rangle_{22}/\overline{uv}$ conditional contribution at the moving probe initially falls off rapidly for $y/\delta<0.1$ (Fig.6(b)). The $\langle uv\rangle_{42}/\overline{uv}$ contribution is consistently smaller across the entire boundary layer, while interactive motions exhibit increased contribution in the vicinity of the stationary probe. The $\langle uv\rangle_{44}/\overline{uv}$ contribution falls off rapidly (Fig. 6(d)) for $y/\delta<0.1$ while it decrease gradually for larger r_2 separations becoming smaller than $\langle uv\rangle_{24}/\overline{uv}$ for $y/\delta>0.35$.

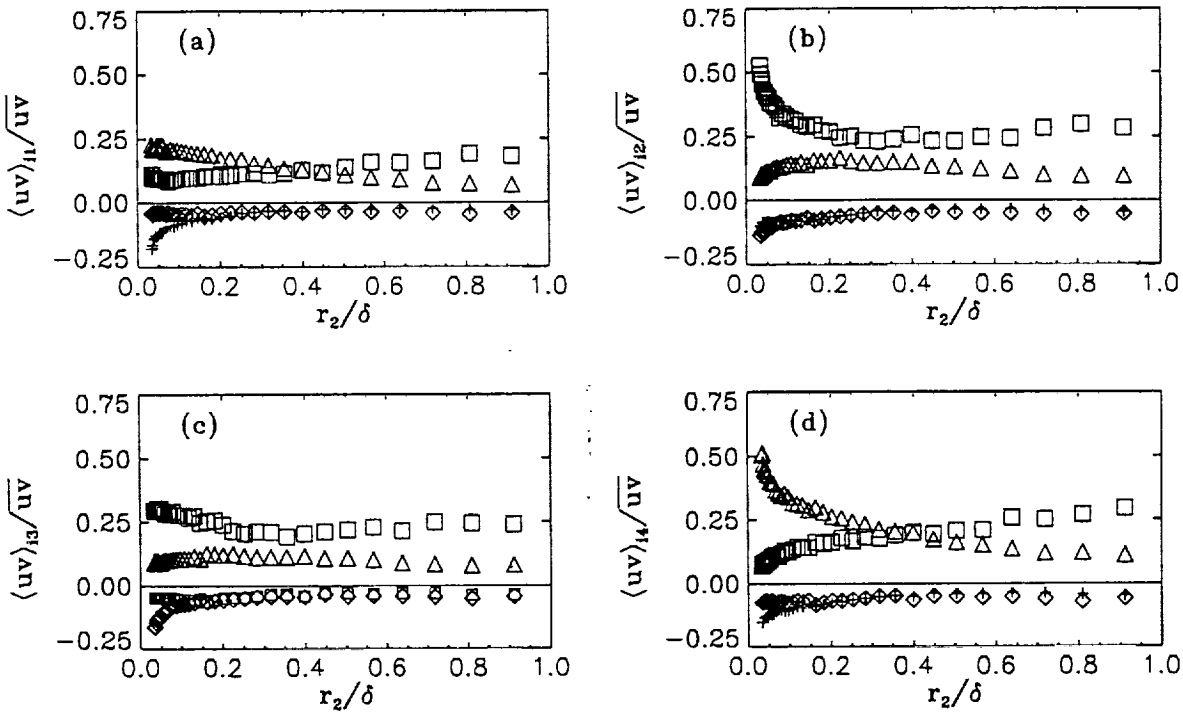

Figure 6. Conditional contribution of different quadrants to the shear stress providing that: (a) Q_1 has occurred at the fixed probe location $y/\delta=0.012$, (b) Q_2, (c) Q_3, (d) Q_4. Symbols:+, Q_1; ❑, Q_2; ◊, Q_3; Δ, Q_4.

It appears that the negative contribution, $\langle uv\rangle_{14}/\overline{uv}$, increases for small values of y giving support for the "splat" effect. The analysis of the conditional quadrant contribution was performed for an instantaneous velocity field at two points in space. However, having in mind that the postulated structure is a 3-D structure inclined in the streamwise direction, a similar analysis is now under way using a time shift between signals at two different spatial locations.

4. CONCLUSIONS

The structure of the recovering turbulent boundary layer perturbed by a back-

ward-facing step was investigated experimentally using two-point two-component velocity measurements. General similarity of the measured spatial correlations with those of Grant (1957) and Tritton (1967) suggested that the characteristic structure is similar to the attached eddies in the near-wall layer and to the double-roller eddy in the outer layer as proposed by Townsend (1976). The two characteristic structures present in TBLs can be connected into a hairpin structure as supported by many other studies. The observed organized structure of the recovering boundary layer appears to have larger dimensions in the two cross flow directions when compared to an undisturbed flat plate TBL. The conditional quadrant analysis of the shear stress suggests that Q_2 and Q_4 are dominating mechanisms in the recovering TBL. In addition, it appears that the interactive motions, Q_1 and Q_3, are produced by the "splatting" of sweep motions and deflection of ejection motions respectively.

ACKNOWLEDGEMENTS

This research was supported by NASA Grant NCC2-465 which is gratefully acknowledged. The hospitality of S. Davis and help by the FML stuff are gratefully acknowledged.

5. REFERENCES

1. Bakewell, H and Lumley,J.L. 1967 *The Physics of Fluids*, Vol. **10**, No. 9.
2. Brown, L.G. and Thomas, A.S.W. 1977 *The Physics of Fluids*, Vol. **20**, No. 10, Put II, S243.
3. Favre, A.J., Gaviglio,J.J. and Dumas, R. 1957 *J. Fluid Mech.* **2**, 313.
4. Grant, H.L. 1958, *J. Fluid Mech.*, **4**, 149.
5. Head, M.R. and Bandyopadhyay, P. 1981 *J. Fluid Mech.*, **107**, 297.
6. Jovic, S. and Browne, L.W.B. 1989, *Tenth Australasian Fluid Mechanics Conference,* University of Melbourne, Melbourne, December 11-15.
7. Jovic, S. and Browne, L.W.B. 1990 *Engineering Turbulence Modelling and Experiments Proceedings of the International Symposium on Engineering Turbulence Modelling and Measurements*, September 24-28, Dubrovnik, Yugoslavia, ed. W. Rodi and E.N. Ganic.
8. Jovic, S. 1993 *2nd International Symposium on Engineering Turbulence Modelling and Measurements*, May 31- June 2, Florence, Italy (to appear).
9. Kim, J. 1983 *Phys. Fluids,* Vol. **26**, No. 8.
10. Klebanoff, P.S. 1954 National Advisory Committee for Aeronautics, TN. 3178.
11. Lumley, J.L. 1967 *Proceedings of the International Colloquium on the Atmosphere and its Influence on the Radio Wave Propagation* (Doklady Akademia Nauk SSSR, Moscow.
12. Moin, P. and Kim, J. 1982 *J. Fluid Mech.*, **118**, 341.
13. Townsend, A.A. 1976 (and 1956) *The Structure of the Turbulent Shear Flow.* Cambridge University Press.
14. Payne, F.R. 1966 *PhD Thesis*, Pennsylvania State University, University Park.

2nd International Symposium on Engineering Turbulence Modelling and Measurements,
May 31- June 2, 1993, Florence, Italy

An experimental study on the recovery of a turbulent boundary layer downstream of the reattachment

Srba Jovic'

Eloret Institute, 3788 Fabian Way, Palo Alto, CA 94303

Abstract

Transport characteristics of the turbulent kinetic energy, k, the shear stress, $-\overline{uv}$, mixing length, l, and eddy viscosity, ν_t, were studied in an incompressible turbulent boundary layer downstream of the reattachment of the separated flow behind a backward-facing step. The Reynolds number, R_h, based on the step height, h, was 37000 and the upstream oncoming flow was a fully developed turbulent boundary layer with R_θ = 3600. Hot-wire measurement techniques were used to measure three Reynolds stresses and higher-order mean products of velocity fluctuations. It was found that downstream of approximately $20h$ the structure of the evolving flow near the wall attains local energy quasi-equilibrium. Recovery of the turbulent structure in the outer part of the flow is much slower and the memory of the upstream perturbation is still traceable even in the last measuring station of $51h$.

1. INTRODUCTION

Separated/reattached flows occur in wide variety of practical engineering applications and therefore has attracted attention of many researchers. This type of flow deviates strongly from an equilibrium turbulent flow structure. The fully developed turbulent structure of the upstream boundary layer is perturbed by a discontinuity in the boundary condition. A non-slip and impervious wall abruptly ends at the step lip allowing the internal mixing layer, imbedded in the turbulent boundary layer, to develop further downstream. The structure of the separated shear layer as it evolves downstream strongly resembles that of a plane-mixing layer. However, this mixing-layer encounters a solid and impervious wall in the reattachment region when it gradually begins to change its character and undergoes transformation to a structure characteristic of a regular TBL. The response of the turbulent structure to the imposed perturbation is not instantaneous across the entire flow but is achieved rather gradually both in space and time. Three different basic flow structures, namely mixing-layer, wall and wake-layer like structures of an ordinary TBL, compete in the recovery region. Depending upon boundary conditions in different flow regions one of the three flow structures prevails. It appears that rates of recovery in the near-wall and outer flow regions are quite different downstream of the reattachment as indicated by Jovic' & Browne (1990). The turbulent structure near the wall recovers much faster then that of in

the outer part of the flow. The fundamental complexities of the turbulent structure of this family of turbulent flows presents a real challenge for the available turbulence models.

Numerous studies have been conducted on separated/reattached flows during the past four decades. The research has been conducted for many different geometric configurations. However, most of these studies have addressed backward-facing step induced separation.

Extensive studies on separated flow for a blunt plate have been made by Cherry, Hiller & Latour (1984) and Kiya & Sasaki (1983,1985). Ruderich & Fernholz (1986), Castro & Hague (1987) and Cutler & Johnston (1989) studied the structure of a separated flow behind a normal plate (fence) with a splitter plate. Chandrsuda & Bradshaw (1981), Kim, Kline & Johnston (1980), Westphal, Johnston & Eaton (1984), Eaton & Johnston (1982), Pronchick & Kline (1983), Driver & Seegmiller (1983), Adams & Johnston (1988), just to name a few, have conducted extensive measurements of a separated flow behind a backward-facing step.

The objective of the present experiment is to present a detailed analysis of the evolution of the transport mechanisms of turbulent kinetic energy, shear stress, mixing length and eddy viscosity in the recovery region of the attached boundary layer downstream of the reattachment point. Important implications pertaining to turbulence models are presented.

2. APPARATUS, TECHNIQUES AND CONDITIONS

The measurements were performed in a wind tunnel comprised of a symmetric three-dimensional 9:1 contraction, a 169 *cm* long flow development section with dimensions 19.7 *cm* x 42 *cm*, a backward-facing step of the height, h, of 3.8 *cm* and width of 42 *cm* and a 205 *cm* long recovery section. The flow was tripped at the inlet of the development section using 1.6 *mm* diameter wire followed by a 110*mm* width of 40 grit emery paper. The side walls diverged slightly outwards to assure approximate zero-pressure gradient in the development and the recovery sections of the tunnel. All the measurements were made at a flow speed, U_{ref}, of 14.7 m/s. The free stream turbulence intensity was 0.4%. The boundary layer measured 40*mm* upstream of the step was fully turbulent having a Reynolds number based on the momentum thickness, R_θ, of 3600 and a shape factor, H, of 1.4.The boundary layer thickness, $\delta_0 \equiv \delta_{99}$, was 31 *mm* resulting in $\delta_0 / h = 0.8$. This perturbation can be classified as a strong perturbation (Bradshaw & Wong (1972)). The aspect ratio (tunnel width/step height) of 11 is just above the value of 10 recommended by de Brederode & Bradshaw (1972) as the minimum to assure two-dimensionality of the flow in the central region of the tunnel. An expansion ratio was 1.19 and the Reynolds number based on the step height was 37000. The pressure gradient in the recovery region for $x > 9h$, is negligibly small. The maximum non-dimensional pressure parameter, $(\nu/\rho u_\tau^3)\, dp/dx$, in this region has a value of about -0.004 which shows that the structure of the reattached flow evolves in a virtually zero-pressure gradient environment.

Mean velocity and turbulence measurements were made with normal and X-wire probes driven by an in-house built constant-temperature anemometers.

The sensor filaments were made of 10% Rhodium-Platinum wire 2.5 μm in diameter and 0.6 mm (or 22 in wall units in the upstream boundary layer) in length for the X-wire probe, and 1.25 μm in diameter and 0.3 mm (or 11 wall units) in length for the normal-wire probe. The spacing between crossed wires was 0.4 mm or 15 wall units. The aspect ratio, l/d, of the sensor filaments was 240 for both probes. The usual 90° included angle of the crossed wires was replaced by the 110° angle. This angle is chosen to improve accuracy of the measurements in the regions with higher levels of local turbulence intensity. The constant temperature anemometers were operated at overheat ratios of 1.3 with a frequency response of $25kHz$ as determined by the square wave test. The normal-wire signal was low-pass filtered at $10kHz$ and was digitized at 20 ksamples/sec for 30 sec. The X-wire signals were low-pass filtered at $6kHz$ and were sampled at 12 ksamples/sec for 30 sec. Analog signals were digitized using a Tustin A/D converter with 15 bit (plus sign) resolution. The probes were calibrated using a static calibration procedure and calibration data of each hot-wire channel were fitted with a fourth order polynomial.

3. RESULTS

3.1 Transport of the turbulent kinetic energy

A low viscosity oil was used to visualize the flow pattern in the separated region and to determine the mean reattachment length. The reattachment line is not a straight line in the spanwise direction but curves upstream near the side walls. Flow reattachment occurs at about $x/h = 6.84$ in the mid plain of the wind tunnel.

The balance of the turbulence kinetic energy in three characteristic streamwise locations ($9.87h$, $20.29h$ and $38.55h$) is shown in Figure 1. Distributions in other seven additional locations are not shown for brevity but will be used in the discussion below. The turbulent kinetic energy equation for two-dimensional flows may be written as follows:

$$U\frac{\partial k}{\partial x} + V\frac{\partial k}{\partial y} = -\frac{\partial}{\partial x}\overline{u\left(k+\frac{p}{\rho}\right)} - \frac{\partial}{\partial y}\overline{v\left(k+\frac{p}{\rho}\right)} - \left(\overline{u^2}-\overline{v^2}\right)\frac{\partial U}{\partial x} - \overline{uv}\frac{\partial U}{\partial y} - \varepsilon$$

Contribution by fluctuating pressure-velocity covariances to the turbulent transport (diffusion term) is typically small in wall bounded flows and was therefore neglected. However, this approximation may be quite crude in the reattachment region of separated flows where large pressure and velocity fluctuations take place. All terms of the transport equation were evaluated from the measured turbulent quantities except the rate of dissipation, which was obtained by difference of all the other terms. Since the spanwise velocity component was not measured, the following approximations are introduced. The turbulent kinetic energy, k, was approximated by 0.75 $(\overline{u^2} + \overline{v^2})$, turbulent diffusion in the streamwise direction, $\overline{uk}$, and in the transverse direction, $\overline{vk}$, were approximated by 0.75 $(\overline{u^3} + \overline{uv^2})$ and 0.75 $(\overline{u^2}\overline{v} + \overline{v^3})$ respectively.

Downstream of reattachment the flow accelerates close to the wall and undergoes structural adjustments to the new boundary condition. Apparently, the flow

is far from being in energy equilibrium as can be seen from Figure 1(a). The flow does not attain equilibrium neither near the wall nor in the outer part of the flow. It was found that a contribution from the three terms, longitudinal turbulent diffusion, $\partial(\overline{uk}) / \partial x$, production by the normal stresses, $-(\overline{u^2} - \overline{v^2})\, \partial U / \partial x$, and the mean flow transport are significant downstream of reattachment which contrasts a regular TBL where contributions by these three agents are negligibly small.

In the early stages of the flow recovery, $x < 12h$, the loss of turbulent energy to

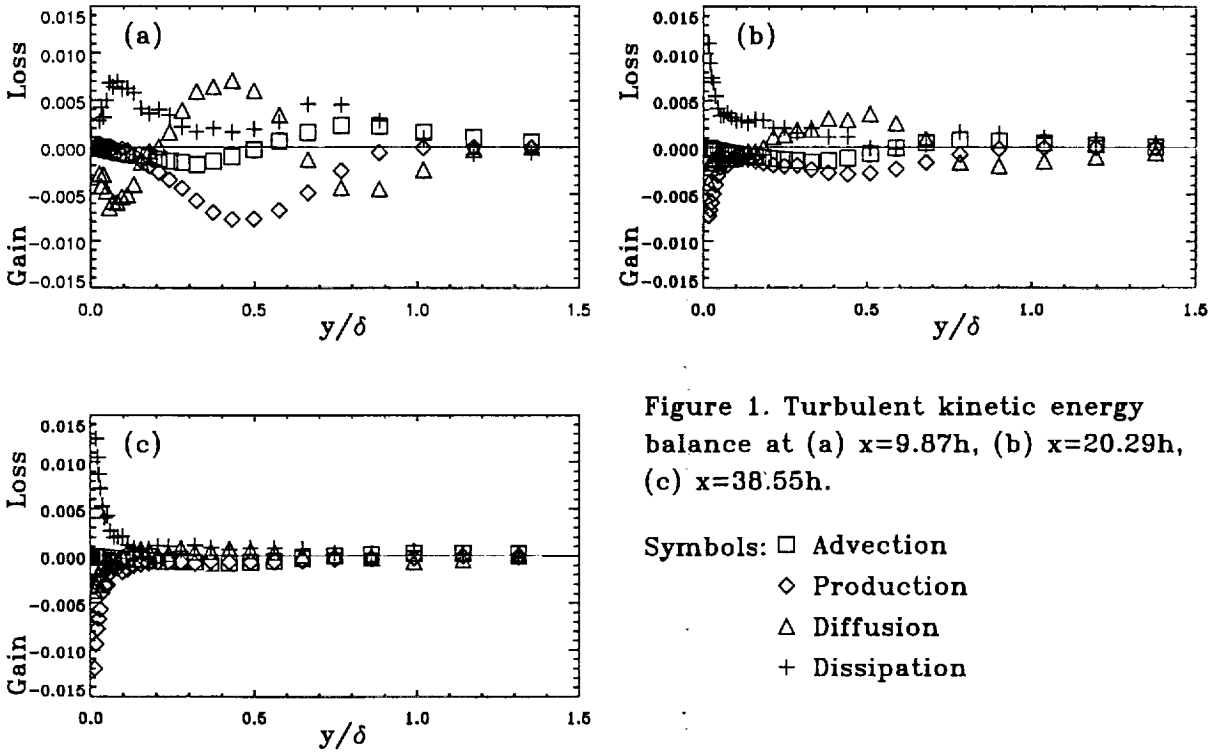

Figure 1. Turbulent kinetic energy balance at (a) x=9.87h, (b) x=20.29h, (c) x=38.55h.

Symbols: □ Advection
◇ Production
△ Diffusion
\+ Dissipation

dissipation in the inner part of the flow, $y < 0.1\delta$, is balanced by the turbulent diffusion (see Fig. 1(a)). It is seen that the contribution of the turbulent energy by the production and convection are negligibly small in this part of the flow. Production by the normal stresses near the wall is negative since velocity derivative $\partial U / \partial x$ is positive due to the flow acceleration and $\overline{u^2}$ is larger then $\overline{v^2}$. This negative production of turbulence energy is canceled by the positive production $-\overline{uv}\, \partial U / \partial y$. These features lead to a conclusion that turbulence models which use equilibrium concepts are not applicable in this region. Note that the k-equation terms shown in Figure 1 were made dimensionless by U_e^3/δ where Ue is a boundary layer edge velocity and δ is a local boundary layer thickness.

The distributions of all the terms of the k-equation in the outer portion of the flow strongly resemble the distributions of the same terms in an ordinary plane mixing layer. Even though the magnitude of each term reduces in the downstream direction, this similarity is retained even up to about $20h$. This shows that the mixing-layer like structure is still present, but decays gradually in the outer part of the flow. On the other hand, the competing wake-like structure of a regular TBL asserts its presence through the boundary condition u=0 and v=0 at the wall. It

affects the mean-velocity gradients, production of turbulence and the turbulent transport through the confinement and break up of large eddies produced at separation. As a result, the peak of the production shifts from the central region of the layer to the wall region where the velocity gradient begins to dominate and the shear stress gradually increases. Transport by the turbulent diffusion gradually decays in the outer region (see Figures 1(b), (c)) while its maximum moves also to the wall region.

The peak of turbulent diffusion in the central region of the flow occurs approximately at 0.45δ. The peak of the diffusion is surprisingly large and represents a significant ratio of the production peak of about 0.85. Apparently, large eddies transfer turbulent energy from the central, the energy rich, region toward the wall and outwards to the boundary layer edge as can be seen in Figures 1.(a), (b). The data suggest that any correct prediction of the separated/reattached flow requires an accurate model for the diffusion terms.

The production peak occurs at about 0.45δ in the transverse direction and dominates the wall production by about $15h$. Downstream of this location, the production in the wall region rapidly increases. It appears that the competing outer layer/mixing-layer like structure ceases to affect wall structure by about $x=20h$ when the familiar wall mechanisms prevail in the production of the wall turbulence. By the streamwise distance of about $x = 30h$, the transport terms of the turbulent kinetic energy further decrease in the outer part of the flow as seen in Fig. 1(b) and 1(c), gradually approaching the structure of a regular TBL.

3.2 Transport of the shear stress

The balance of the shear stress, $-\overline{uv}$, in three streamwise locations ($9.87h$, $20.29h$ and $38.55h$) is shown in Figure 2. The shear stress transport equation for two-dimensional flows may be written as follows:

$$U\frac{\partial -\overline{uv}}{\partial x} + V\frac{\partial -\overline{uv}}{\partial y} = \frac{\partial}{\partial x}\left(\overline{u^2 v - \frac{p}{\rho}v}\right) + \frac{\partial}{\partial y}\left(\overline{uv^2 - \frac{p}{\rho}u}\right) + \overline{v^2}\frac{\partial U}{\partial y} + \overline{u^2}\frac{\partial V}{\partial x} - \overline{\frac{p}{\rho}\left(\frac{\partial u}{\partial y} + \frac{\partial v}{\partial x}\right)}$$

The turbulent diffusion due to pressure and velocity correlation, $\partial(\overline{vp/\rho}) / \partial x$ and $\partial(\overline{up/\rho}) / \partial y$, and the production term by the normal stress $\overline{u}^2$ $(\partial V / \partial x)$ were neglected. Note that the shear stress transport equation terms shown in Figure 2 were made dimensionless by U_e^3/δ. The advection term is smaller than for the k-equation (see Figs 1 and 2). The three terms which dominate transport mechanism are production, $\overline{v}^2$ $(\partial U / \partial y)$, combined longitudinal and transverse turbulent diffusion and the pressure-strain term. In the central portion of the flow, maximum of the shear stress production occur at the same location as the production of the turbulent energy. The gain of the shear stress by the production is balanced by the large turbulent diffusion term and the pressure-strain term. The gain by diffusion and the loss by the pressure-strain term are not balanced in the near-wall region as would be expected based on the k-equation behavior near the wall. The diffusion term is of the same magnitude and sign as the production term in the wall region. The production of the shear stress has significantly increased near

the wall by $x=20h$ (see Fig. 2(b)). Distributions of diffusion and pressure-strain terms in the wall region resemble the regular TBL by $30h$ which is consistent with the behavior of the k-equation. In the outer part of the flow, all three terms decrease significantly beyond $30h$ so that by $x=38.55h$ (see Figure 2(c)) the distribution of all terms strongly resembles that of a regular TBL.

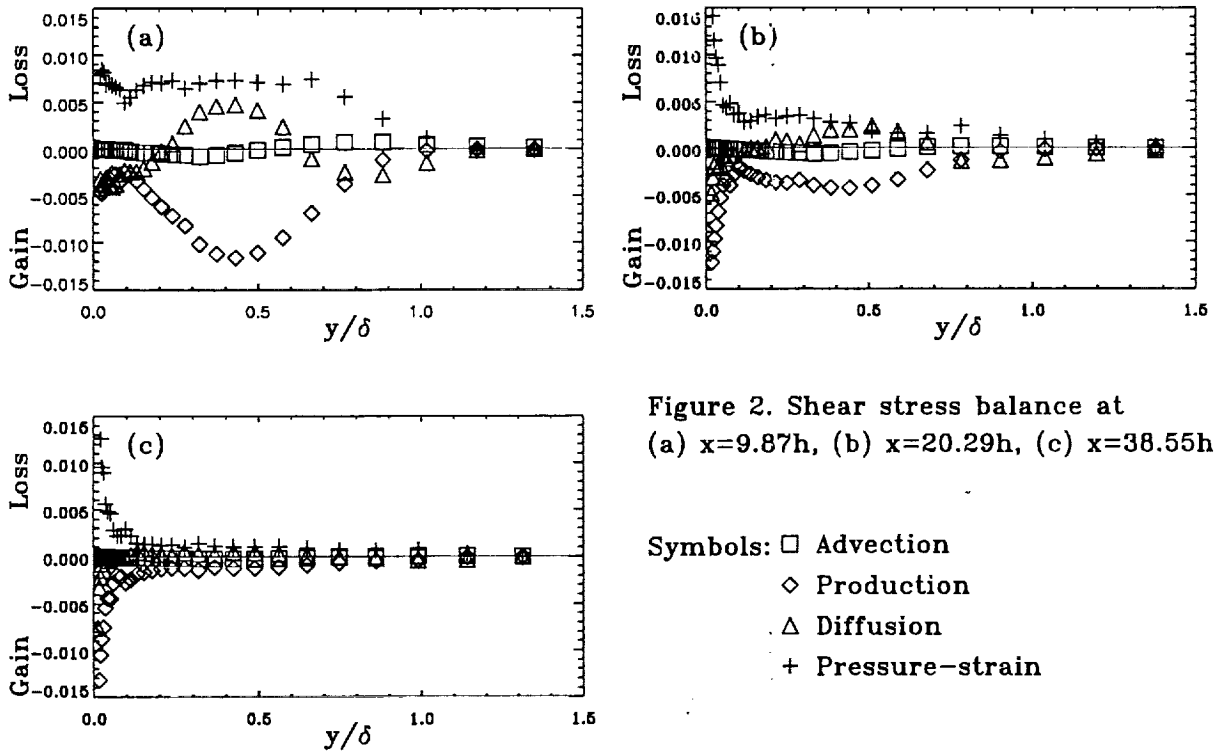

Figure 2. Shear stress balance at (a) x=9.87h, (b) x=20.29h, (c) x=38.55h

Symbols: □ Advection
◇ Production
△ Diffusion
\+ Pressure–strain

3.3 Derived quantities and their implications for modeling

Stream line curvature was neglected in the recovery region, and the shear stress and mean streamwise velocity, which were measured in the Cartesian coordinate system, were used to evaluate Prandtl's mixing length, $l = \sqrt{-\overline{uv}}/(\partial U/\partial y)$, and eddy-viscosity, $\nu_t = -\overline{uv}/(\partial U/\partial y)$. These two turbulence concepts have been successfully used in calculating slowly evolving flows. However, these simple models fail in more complex flow configurations, such as separated/reattached flows, where the Reynolds stresses respond slowly to the rapid changes of the rate of strain.

Non-dimensional mixing-length, l/δ, and eddy-viscosity, $\nu_t / U_e\delta^*$, are shown in Figures 3 and 4 respectively. Distribution of the respective quantities are compared with those of the upstream fully developed TBL. Note that the Reynolds number of the upstream boundary layer of $R_\theta = 3600$ is lower than the one in the recovery region of the flow. The values of the Reynolds number R_θ in the recovery region for the given R_h are typically over 9000.

Near the wall the mixing length is a linear function of the normal distance from the wall. However, the slope is significantly larger than the value of $\kappa = 0.41$ typical for a zero-pressure-gradient equilibrium boundary layer. After reaching a max-

imum value away from the wall (see Fig. 4) the mixing length sharply drops which contrasts its behavior in a regular TBL. The drop indicates presence of two dis-

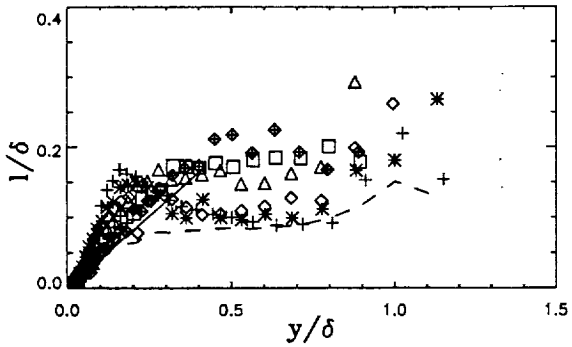

Figure 3. Profiles of the mixing length.

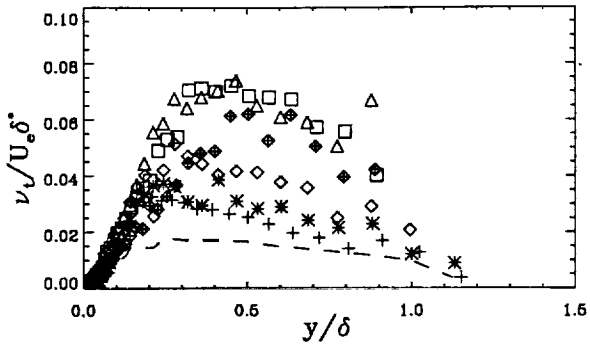

Figure 4. Profiles of the eddy viscosity

Symbols: - -, x/h = -1.05; +,9.21;*,10.53; ◊,13.16; Δ,20.29; ❑,28.76; ◊,51.18; —,0.41y

tinct structures with different origins, one being associated with the developing internal TBL and the second one being associated with the inherited mixing-layer like structure in the outer part of the flow. The slope of the linear inner region gradually decreases with downstream distance. The slope versus x/h is presented in Figure 5. It is remarkable to see that the slope has not fully recovered even at $x = 51h$ despite the observed approximate local energy equilibrium near the wall. More careful examination of Figures 1(b) and 1(c) shows that the turbulent diffusion is quite large near the wall. Further more, the advection and the turbulent diffusion terms are not negligible in the outer layer downstream of $30h$. This leads to the conclusion that the flow still behaves as a non equilibrium shear layer.

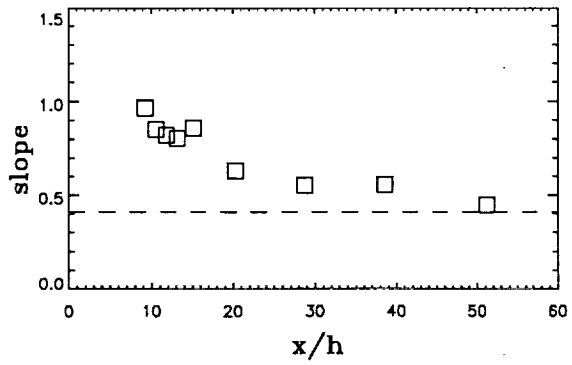

Figure 5. Mixing length slope variation vs. x/h.

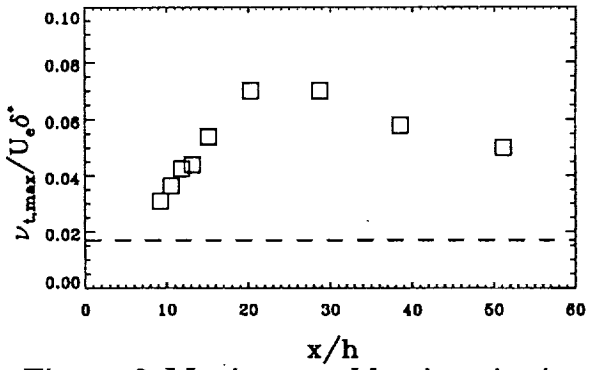

Figure 6. Maximum eddy viscosity in variation vs. x/h.

Dashed line denotes the value of 0.41 in Fig. 5 and the value of 0.017 in Fig. 6.

The values of the mixing length in the outer part of the flow exceeds the constant value of 0.085 characteristic of a zero-pressure gradient equilibrium TBL. The mixing length gradually increases approaching approximately a constant value of about 0.19 in the outer region for $x > 30h$. It appears that the turbulent

structure reaches a quasi-equilibrium state in the outer part of the flow leading to the possible conclusion that the wake-boundary-layer like structure prevails over the mixing layer like structure.

Similarly, the eddy-viscosity, ν_t / $U_e\delta^*$, deviates both in the wall and the outer flow regions from the distribution of the upstream TBL (see Fig. 4). It appears that the slope near the wall, like in the case of the mixing length, is larger then that of the upstream TBL. The slope gradually decreases downstream approaching the value of κu_τ (u_τ is a local shear velocity). Maximum values of the normalized eddy viscosity are shown in Figure 6. It is seen that the eddy-viscosity in the outer part of the flow rises initially reaching the value of 0.075 at approximately $x = 20h$. Subsequently, it begins to decay at a very slow rate. It is seen that even at the last measuring station of $x = 51h$ the maximum eddy viscosity is about four times larger than the value of 0.017 in an equilibrium TBL.These high values of the mixing length and eddy viscosity in the outer parts of the flow far downstream indicate the lag of Reynolds stresses response to the mean rate of strain. However, a recovery trend can be clearly observed.

4. CONCLUSIONS

The results presented and discussed in the previous sections led to the following conclusions about the recovering turbulent structure of the flow downstream of the reattachment point.

For a Reynolds number of R_h = 37000 and an upstream boundary layer thickness $\delta = 0.8h$ most of the flow recovery downstream of the reattachment is achieved by about $30h$ or about three mean reattachment lengths downstream of the reattachment point. Further downstream recovery is a very slow process especially in the outer flow region. The thin-shear layer approximation is inapplicable in the recovery region of a separated TBL. Longitudinal turbulent diffusion and production of the turbulent energy by the normal stresses play an important role in the balance of the turbulent kinetic energy transport equation. Turbulent diffusion and dissipation are balanced in the near-wall part of the flow up to about $x=15h$, suggesting that energy equilibrium concepts of turbulence modeling are not applicable in this region. It appears that energy equilibrium is only approximately achieved in the near-wall region for $x > 20h$ due to still large turbulent diffusion near the wall. This quasi-equilibrium state of the flow structure leads to a linear distribution of the mixing length and eddy viscosity in the wall region. The slopes are, however, larger than the von Karman constant, $\kappa = 0.41$, for the mixing length and κu_τ for the eddy viscosity. Mixing length and eddy viscosity in the outer part of the flow exceed the values of a regular TBL up to four times even at the last measuring station.

ACKNOWLEDGMENTS

This research was supported by NASA Grant NCC2-465. The author is indebted to J. Marvin and D. Driver for their continuous encouragement throughout the experiment. Helpful discussions with P. Bandyopadhyay are also gratefully acknowledged.

5. REFERENCES

1. Adams, E.W., Johnston, J.P. & Eaton, J.K. 1984, Experiments on the structure of a turbulent reattaching shear layer. Rep. MD-43, Thermosciences Div., Dept. of Mech. Eng., Stanford University, CA.
2. Bradshaw, P. & Wong, F.Y.F. 1971, The Reattachment and relaxation of a turbulent shear layer. *J. Fluid Mech.* **52**, 113.
3. Chandrsuda, C. & Bradshaw, P. 1981, Turbulence structure of a reattaching mixing layer. *J. Fluid Mech.* **110**, 171.
4. Castro, I.P. & Haque, A. 1987, The structure of a turbulent shear layer bounding a separation region. *J. Fluid Mech.* **179**, 439.
5. Cherry, N.J., Hiller, R. & Latour, M.E.M.P. 1984, Unsteady measurements in a separated and reattaching flow. *J. Fluid Mech.* **144**, 13.
6. Cutler, A. & Johnston, J.P. 1989, The relaxation of a turbulent boundary layer in an adverse pressure gradient. *J. Fluid Mech.* **200**, 367.
7. Driver, D.M. & Seegmiller, H.L. 1985, Features of a reattaching shear layer in a divergent channel flow. *AIAA J.* **23**, 163.
8. Eaton, J.K. & Johnston, J.P. 1982, Low frequency unsteadiness of a reattaching turbulent shear layer. In *Turbulent Shear Flows 3* (ed. L.J. Bradbury, F. Durst, B.E. Launder, F.W. Schmidt & J.H. Whitelaw), p. 162. Springer-Verlag.
9. Kim, J., Kline, S.J. & Johnston 1980, Investigation of a reattaching turbulent shear layer: Flow over a backward-facing step. *Trans. ASME, J. Fluids Engrg.* **102**, No. 3, 302.
10. Jovic′, S. and Browne, L.W.B. 1990, Turbulent heat transfer mechanism in a recovery region of a separated flow. *Engineering Turbulence Modeling and Experiments Proceedings of the International Symposium on Engineering Turbulence Modelling and Measurements*, September 24-28, ed. W. Rodi and E.N. Ganic′.
11. Kiya, M. & Sasaki, K. 1983, Structure of a turbulent separation bubble. *J. Fluid Mech.* **137**, 83.
12. Kiya, M. & Sasaki, K. 1985, Structure of large-scale vortices and unsteady reverse flow in the reattaching zone of a turbulent separation bubble. *J. Fluid Mech.* **154**, 463.
13. Pronchick. S.W. & Kline, S.J. 1983, An experimental investigation of the structure of a turbulent reattaching flow behind a backward-facing step. Report MD-42, Thermosciences Div., Mech. Eng. Dept., Stanford University.
14. Ruderich, R. & Fernhholz, H.H. 1986, An experimental investigation of a turbulent of a turbulent shear flow with separation, reverse flow and reattachment. *J. Fluid Mech.* **163**, 283.
15. Westphal, R.V., Johnston, J.P. & Eaton, J.K. 1984, Experimental study of flow reattachment in a single-sided sudden expansion. NASA CR-3765.